ELSEVIER

Journal of Alloys and Compounds 317–318 (2001) 612–618

Journal of ALLOYS AND COMPOUNDS

www.elsevier.com/locate/jallcom

On the kinetics of chromium electrodeposition on copper electrodes

P. Baraldi[a,*], E. Soragni[a], C. Fontanesi[a], V. Ganzerli[b]

[a]*Dipartimento di Chimica Università di Modena e Reggio Emilia, Via Campi 183, 41100 Modena, Italy*
[b]*Oleo Component System O.C.S. s.r.l., Via Salvemini 26, 41100 Modena, Italy*

Abstract

In a previous work, we observed that, during cyclic potentiodynamic curves of cathodic polarisation (from 0.00 to −1.25 V/SCE, 5 mV s^{-1}) in chromic acid solution of industrial composition, ARMCO iron undergoes a pitting corrosion, while carbon steels undergo a selective ferritic corrosion. Blisters of pure iron were also observed on ARMCO iron electrodes surface. These occurrences suggest a direct participation of the metal substrate to the overall reaction of reduction of the chromic acid to chromium metal. Therefore, the chemical nature of the electrode metal has been changed, in order to prove that the chromium reduction goes on through an *ECE* mechanism involving a fast chemical reaction between unstable intermediate chromium products and the metal substrate. Cathodic potentiodynamic polarisation curves were performed on copper electrodes and the scans were stopped at four different potentials (−0.90, −1.00, −1.10 and −1.25 V/SCE). The copper surface undergoes a severe corrosion in all the experimental conditions. The morphology of the attack depends on the polarisation potential and on the presence of additives in solution, like iron sulphate.

Keywords: Chromium; Electrodeposition; Copper; Reaction mechanism

1. Introduction

Chromium coatings are widely used to confer particular mechanical and decorative finishes to metallic parts.

Even if the industrial process has been applied since the Fink's patent [1] was published in 1926, the electroreduction reaction mechanism is not quite clear. Some authors [2,3] rationalised the role played by the sulphate anions proposing a multistep reductive mechanism where the $HCr_3O_{10}^-$ species, which form a complex with sulphate ions, is reduced stepwise to Cr. According to potentiodynamic and microscopic studies on Pt, Pd, Cr and Fe electrodes, others [4–8] suggested and observed the formation of an amorphous film of chromic chromate, $Cr(OH)_3Cr(OH)CrO_4$, following the hydrogen evolution reaction. More negative potentials cause the break down of the film that is replaced by a liquid layer with higher density, perhaps due to a polymerisation reaction of the chromic acid. The nature of this dense layer, that would be the 'true' reactant of the chromium reduction reaction, is not yet fully understood.

On the other hand, in a previous work [9], we observed that, during cyclic potentiodynamic curves of cathodic polarisation (from 0.00 to −1.25 V/SCE, 5 mV s^{-1}) in chromic acid solution of industrial composition, ARMCO iron undergoes a pitting corrosion, while carbon steels undergo a selective ferritic corrosion. Blisters of pure iron were also observed on ARMCO iron electrodes surface. Together with the analysis of the polarisation curves, these occurrences suggest a direct participation of the metal substrate to the overall reduction reaction of the chromic acid to chromium metal. In particular, an *ECE* mechanism may be suggested: a first electroreduction step, producing unstable intermediate chromium compounds, is followed by a fast chemical step whose products are reduced at higher potentials. The chemical step can involve the metal substrate. In this case the kinetics of the process depends strongly on the potentials of the species involved in the reactions. So, in order to investigate further this subject, we have changed the nature of the metal substrate. The potentiodynamic curves were recorded on commercial copper electrodes in a solution of conventional industrial

*Corresponding author. Tel.: +39-059-205-5087; fax: +39-039-373-543.

E-mail address: pietrob@unimo.it (P. Baraldi).

0925-8388/01/$ – see front matter
PII: S0925-8388(00)01397-9

composition and with the addition of iron sulphate. The results are compared to those obtained on carbon steel electrodes in the same bath and with addition of copper sulphate.

2. Experimental

The potentiodynamic polarisation curves were performed using an EG & G potentiostat/galvanostat model 273 driven by a host computer. Each measurement session is composed by three consecutive cyclic scans (without the renewing of electrode surface) from the rest potential to four different cathodic peak potentials (−0.900, −1.000, −1.100 and −1.250 V (SCE)). The scan rate was kept constant, 5 mV s^{-1}.

A conventional three electrodes electrochemical cell was used; the counter electrode was a lead/antimony alloy ring; the working electrodes were obtained by cutting commercial rods of carbon steels (0.4 and 0.5% C) and copper. The surfaces were mirror finished using alumina powder paste (AP and AF paste, Struers). The specimen disk was mounted in a teflon holder inserted in the cell from the bottom. The exposed surface was 0.5 cm^2 for copper electrodes and 1.0 cm^2 for steel electrodes. The reference electrode was a saturated calomel electrode (SCE).

Solutions were made following a typical industrial plating bath composition: 250 g dm^{-3} CrO_3 (Aldrich), 2.5 g dm^{-3} H_2SO_4 (Carlo Erba R.P.E.). In tests on copper, ferrous sulphate 10^{-4} M was added to the solution, while in those on carbon steel copper sulphate 10^{-2} M was added to the solution keeping constant the sulphuric acid concentration.

For SEM analysis (Philips XL40) the scans were stopped at the potential peak of the first cycle for 1 min, then the specimens were extracted from the solution, washed and dried.

The temperature was controlled and maintained at 50±0.1°C.

3. Results and discussion

In the case of the Cu electrode and pure solution, the *first direct scan* copper curves (Figs. 1–4A, solid line) show a wide current peak made up of a shoulder (0.10–0.12 V) and a maximum (0.02÷0.06 V). After the maximum, the current falls down with large oscillations up

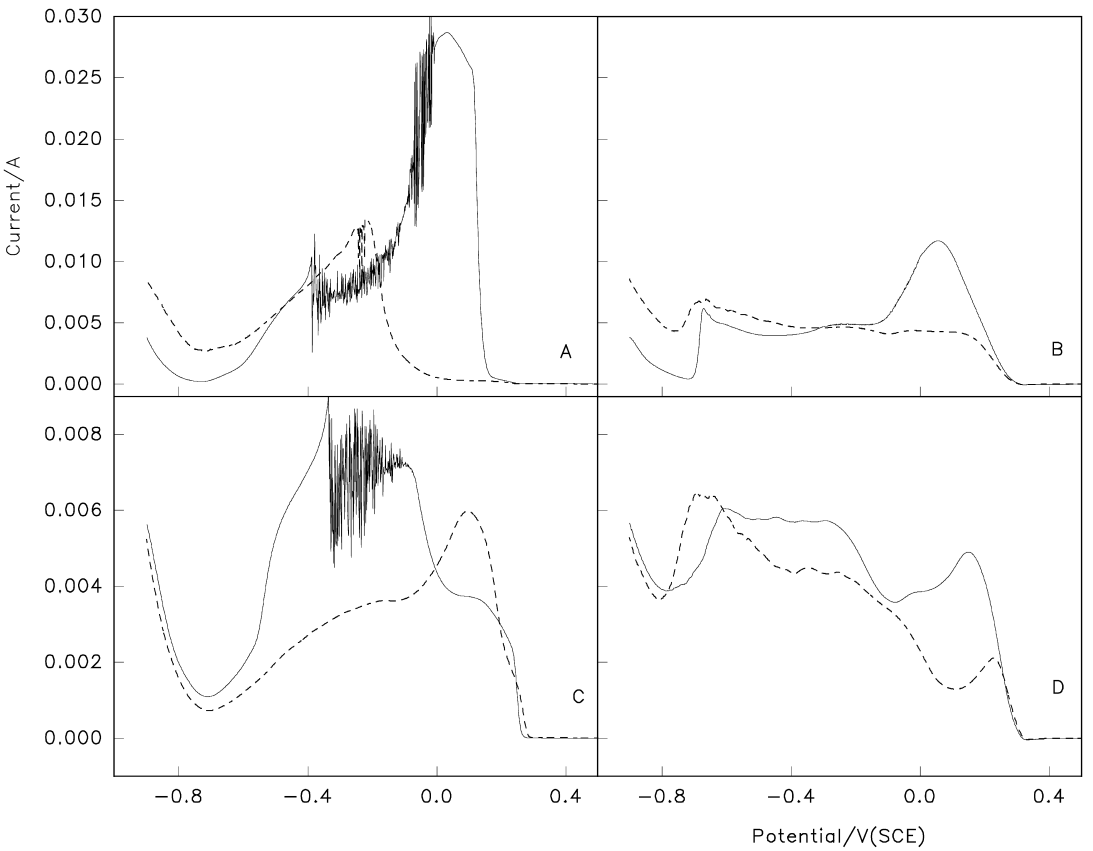

Fig. 1. Potentiodynamic polarisation curves on copper electrode without (solid line) and with (dotted line) addition of iron sulphate, inversion potentials −0.90 V (SCE): (A) first direct scan, (B) first reverse scan, (C) third direct scan, (D) third reverse scan.

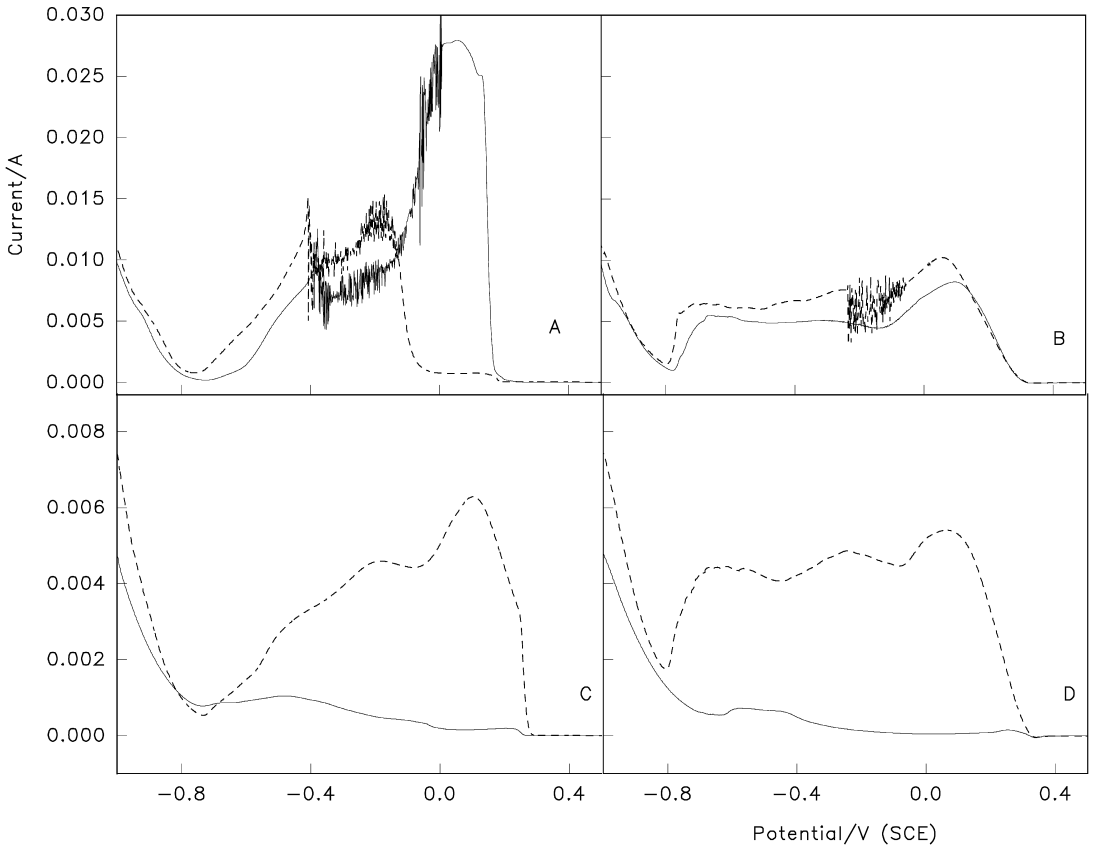

Fig. 2. Potentiodynamic polarisation curves on copper electrode without (solid line) and with (dotted line) addition of iron sulphate, inversion potentials −1.00 V (SCE): (A) first direct scan, (B) first reverse scan, (C) third direct scan, (D) third reverse scan.

to −0.4 V, then it decreases to a deep minimum (~−0.75 V) to increase again because of the starting of chromium deposition. The behaviour of the reverse scans and of the following cycles depends on the values of inversion potential (IP).

For IP of −0.90, −1.00 and −1.10 V, the *first reverse scans* (Figs. 1B, 2B and 3B) preserve about the same behaviour: between −0.70 and −0.65 V, a fast process of desorption appears, this is followed by a potential interval of almost constant current (~0.005 A), in which some 'waves' may be identified. At 0.06÷0.11 V, a broad maximum is present. When IP=−1.10 V, this peak is splitted in two parts: the first one at 0.04 V, the second one, with lower current, at 0.180 V (Fig. 3B); this happens also in the reverse scan of the third cycle, but with current values inverted: the current of the first is lower than the second one and, however, under the plateau current value between −0.6 and −0.2 V.

In the *third direct* scan for the −0.90 V IP (Fig. 1C), the high maximum at positive potential is drastically reduced, but the current oscillations are maintained at the same value of the first direct scan for a potential range from 0.00 to −0.35 V.

At IP of −1.00 V (Fig. 2C and D), both third direct and reverse scans show only 'traces' of the preceding behaviours. At higher IP (Figs. 3C,D and 4C,4D), the curves are quite flat up to the start of the chromium deposition.

This behaviour may be explained assuming that the reduction products are progressively adsorbed on the copper surface and they are stable enough to be electrochemically not reducible at low potentials. Only when the potential increases to values more negative than −1.100 V the reduction takes place.

The behaviours of the carbon steel electrode (0.4% C) in pure solution has been studied in a previous work [10]. Here they are compared with the results obtained with the addition of copper sulphate in solution. For instance, the Fig. 5 shows only the first scans of potentiodynamic curves obtained without (solid lines) and with (dotted lines) copper sulphate addition, at two IP (A: direct scan, B: reverse scan at IP=−1.00 V; C: direct scan, D: reverse scan at IP=−1.25 V). The effect of the copper ions presence is to reduce dramatically the peak current and to shift the start of the chromium reduction to less negative potentials, this fact leads to a higher final current.

Table 1 shows the influence of the iron and copper ions addition on the rest potential: the addition of copper ions does not influence the steel potential, while the addition of iron ions shifts the potential of copper electrode toward less noble values (about 80 mV).

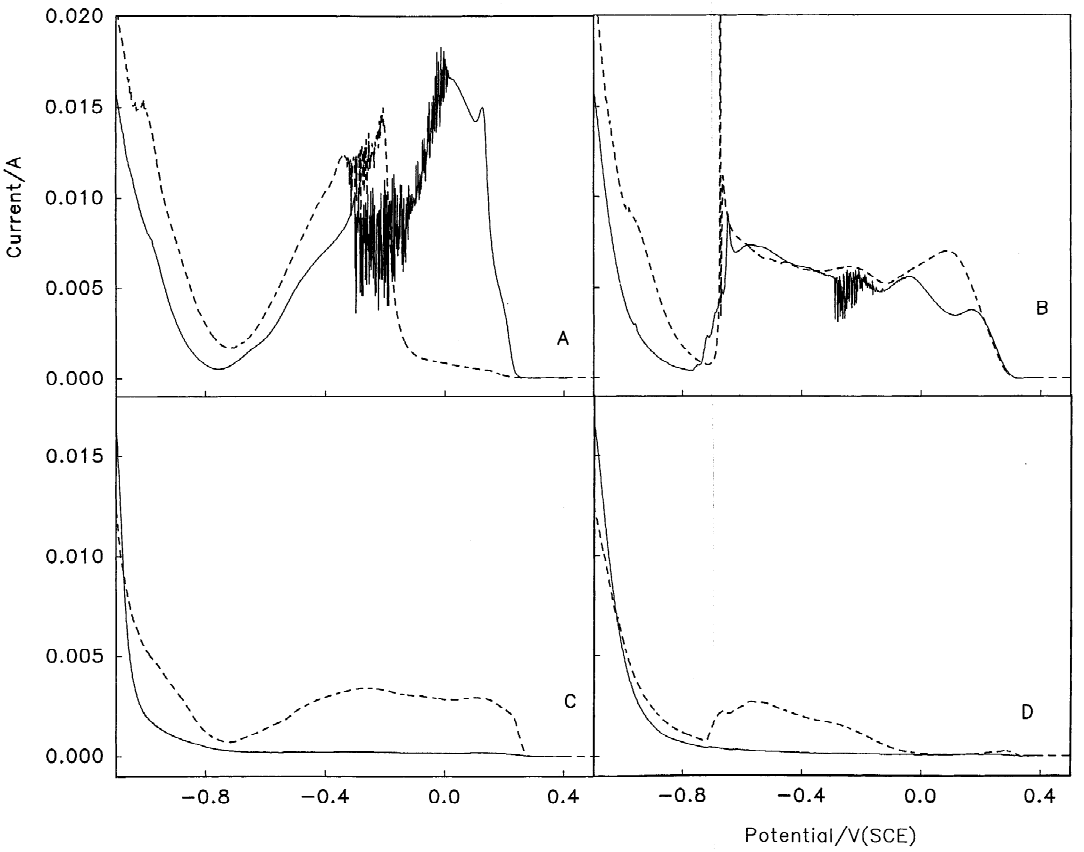

Fig. 3. Potentiodynamic polarisation curves on copper electrode without (solid line) and with (dotted line) addition of iron sulphate, inversion potentials −1.10 V (SCE): (A) first direct scan, (B) first reverse scan, (C) third direct scan, (D) third reverse scan.

The SEM photographs of Figs. 6 and 7 show the surface of the copper after the cathodic polarisation curves. Although from a thermodynamic point of view copper corrodes in oxy-acids, free corrosion tests have shown that it is strongly passivated in chromic acid solution. Actually the copper undergoes a severe corrosion (Fig. 6), which is deeper in solutions containing iron sulphate (Fig. 7). The morphology of the attack depends on the inversion potentials. It is rather important to point out the formation of pyramidal crystals of pure copper (EDAX analysis) at the potential of −1.00 V (Fig. 6B). This fact may be due to a cathodic reduction of the previously dissolved copper, thereby indicating a true participation of copper ions to the overall reaction of chromium reduction. At −1.10 V randomly distributed spots of pure chromium appear (Fig. 6C, white points). At −1.25 V, the surface is quite covered by a thin chromium film. The steel surface is not corroded at low potentials; only at −1.25 V, under the chromium film, the 'weft' of the metal structure is put in evidence by the selective corrosion undergone by the electrode (Fig. 8).

Table 1
Rest potentials of carbon steel and copper electrodes in various solutions

Solution	Electrode potential [V (SCE)]	
	Carbon steel	Copper
Pure solution	0.808	0.617
Cu addition	0.809	–
Fe addition	–	0.535

As for iron [10], the nobler potential assumed by copper electrodes in chromic acid solution may be considered a mixed potential due to a redox reactions mechanism of the following type:

Copper corrosion $2Cu + H_2Cr_2O_7 \rightarrow Cu_2Cr_2O_7 + H_2$

Oxidation $Cu_2Cr_2O_7 + 2H_2O \rightarrow 2CuO + H_2Cr_2O_7 + H^+ + 2e$

Reduction $4H_2Cr_2O_7 + 6\,H^+ + 6e \rightarrow Cr_2(Cr_2O_7)_3 + 7H_2O$

Total reaction $3Cu_2Cr_2O_7 + H_2Cr_2O_7 \rightarrow 6CuO + Cr_2(Cr_2O_7)_3 + H_2O$

Or $3Cu_2Cr_2O_7 + 4H_2Cr_2O_7 \rightarrow 6CuCr_2O_7 + Cr_2O_3 + 4\,H_2O$

According to this reaction scheme, various insoluble or partially soluble products are formed in the adsorbed state,

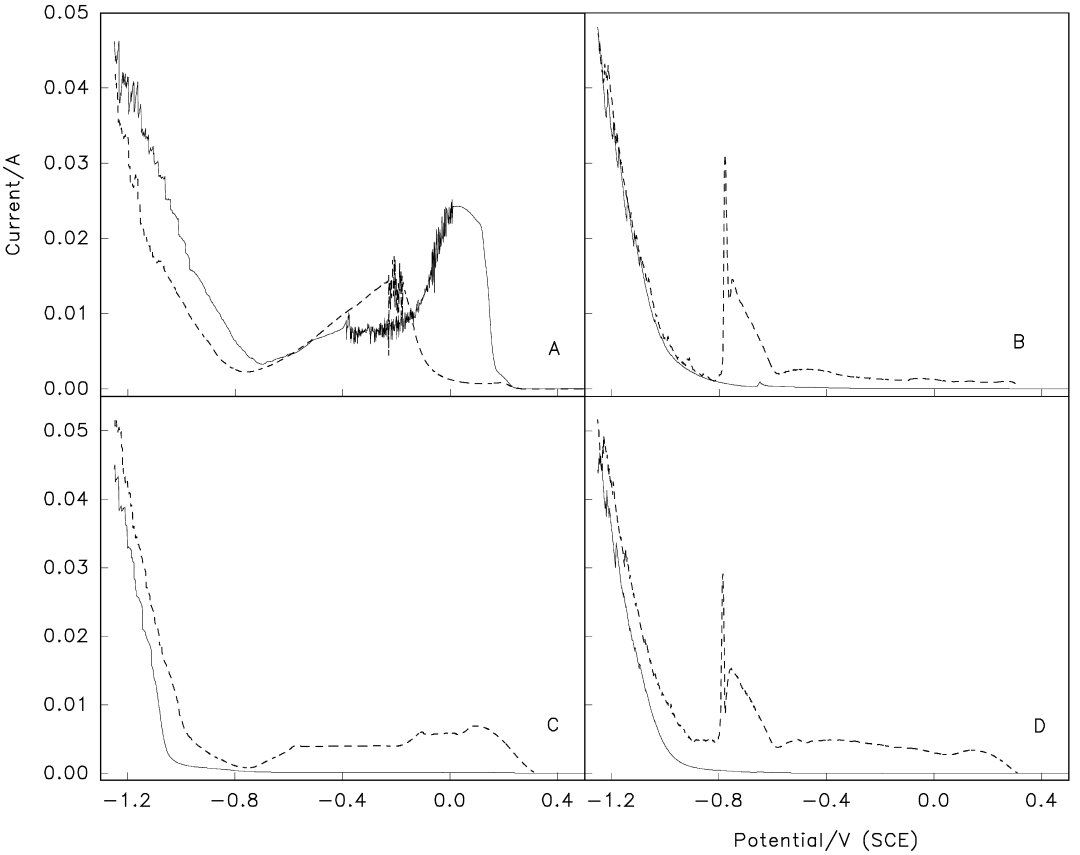

Fig. 4. Potentiodynamic polarisation curves on copper electrode without (solid line) and with (dotted line) addition of iron sulphate, inversion potentials −1.25 V (SCE): (A) first direct scan, (B) first reverse scan, (C) third direct scan, (D) third reverse scan.

thus giving rise to a protecting film that passivates the electrodic metal surface.

This passive film may be reduced during the first cathodic polarisation, and the relevant reduction compounds can react with the chromic acid producing intermediates that are then reduced at less noble potentials. If the species involved in the reduction were chromium oxides, the current peaks would take place at the same potential both on iron and copper electrodes. On copper, the first high current peak is at about 0.100 V/SCE, while on carbon steel it is at −0.400 V/SCE. On the other hand, the analysis of the pH–potential diagrams [11] shows that the standard potentials of copper reactions are always nobler than those of the corresponding iron reactions (Table 2), with the only exception of the aqueous equilibria of the systems Cu^{2+}/Cu^{+} and Fe^{3+}/Fe^{2+}, which standard potentials are −0.088 and 0.530 V/SCE, respectively. This could explain why, on copper, the reduction current peaks occur at nobler potentials. Moreover the oscillations that appear both on copper and carbon steel electrodes, may be due to the formation of temporarily insoluble compounds adsorbed on the metal surface; these compounds block the current until they are dissolved, then the surface becomes again active. At cathodic potentials the copper and iron oxides are stable at high pH (>5), while the pH of plating solution is lower than zero. If the current is stopped by the oxide adsorption, it means that either a local pH increase attends the reduction process or the intermediate reduction products are stable complexes of the chromic acid, which are not reduced at low IP.

The current oscillations on copper electrode reveal the presence of two kind of these compounds, in fact the oscillations may be divided in two potentials ranges (Figs.

Table 2
Comparison between standard potentials of the reduction reactions involving copper and iron calculated for hydroxides [11]

Reactions	Standard potentials V(SCE)
$Fe_2O_3+6H^++2e\rightarrow 2Fe^{2+}+3H_2O$	$0.813-0.177pH-0.059\log(Fe^{2+})$
$CuO+2H^++1e\rightarrow Cu^++H_2O$	$0.379-0.118pH-0.059\log(Cu^{+})$
$Fe_2O_3+6H^++2e\rightarrow 2FeO+H_2O$	$0.030-0.059pH$
$2CuO+2H^++2e\rightarrow Cu_2O+H_2O$	$0.506-0.059pH$
$Fe_2O_3+6H^+\ 6e\rightarrow 2Fe+3H_2O$	$-0.182-0.059pH$
$CuO+2H^++2e\rightarrow Cu+H_2O$	$0.368-0.059pH$
$FeO+2H^++2e\rightarrow Fe+H_2O$	$-0.288-0.059pH$
$Cu_2O+2H^++2e\rightarrow 2Cu+H_2O$	$0.230-0.059pH$
$Fe^{3+}+3e\rightarrow Fe$	$-0.278+0.0197\log(Fe^{3+})$
$Cu^{2+}+2e\rightarrow Cu$	$0.096+0.029\log(Cu^{2+})$
$Fe^{2+}+2e\rightarrow Fe$	$-0.440+0.029\log(Fe^{3+})$
$Cu^{+}+e\rightarrow Cu$	$0.279+0.059\log(Cu^{+})$
$Fe^{3+}+e\rightarrow Fe^{2+}$	$0.530+0.059\log(Fe^{3+}/Fe^{2+})$
$Cu^{2+}+e\rightarrow Cu^{+}$	$-0.088+0.059\log(Cu^{2+}/Cu^{+})$

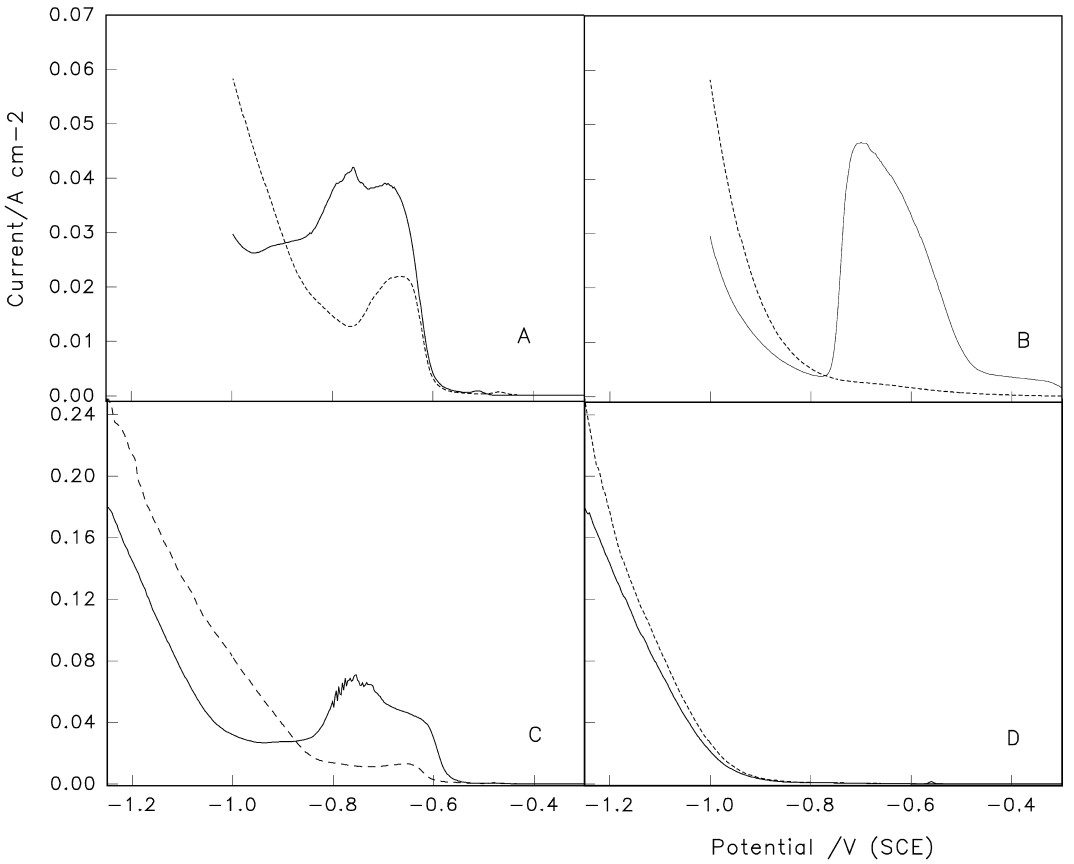

Fig. 5. Potentiodynamic polarisation curves on carbon steel electrode without (solid line) and with (dotted line) addition of copper sulphate, inversion potentials −1.00 V (SCE): (A) first direct scan, (B) first reverse scan; inversion potentials −1.25 V(SCE), (C) first direct scan, (D) first reverse scan.

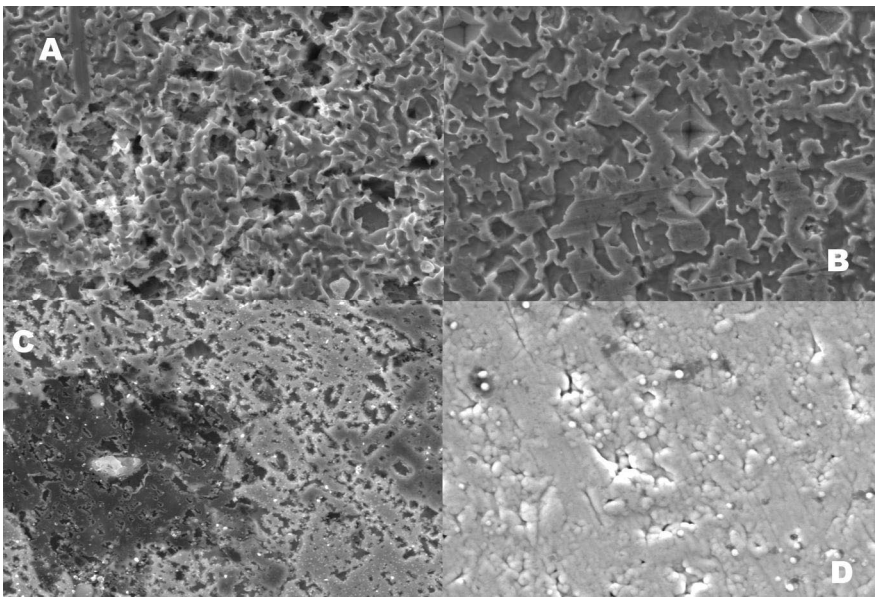

Fig. 6. Morphology of corrosion attack of copper electrode in pure solution at various polarisation potentials: (A) −0.90 V (SCE); (B) −1.00 V; (C) −1.10 V; (D) −1.25 V.

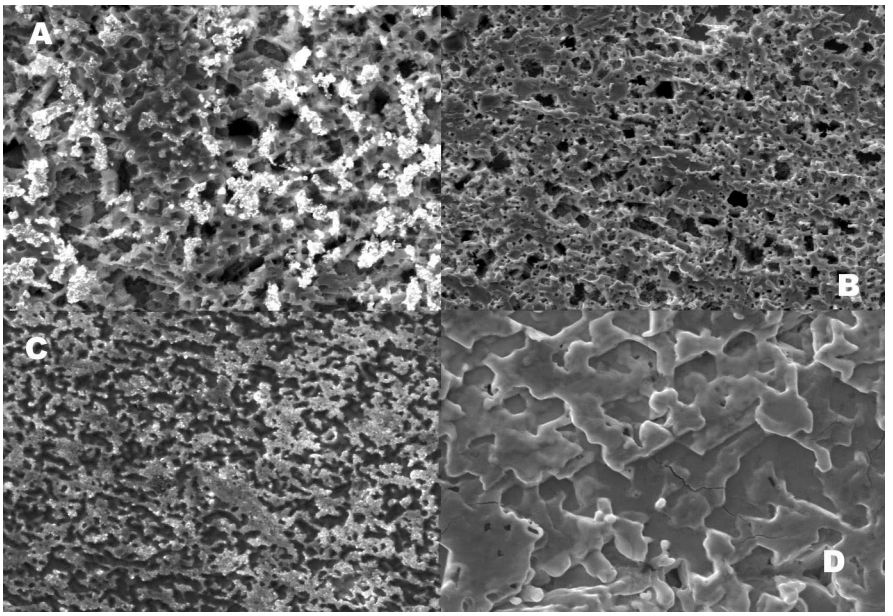

Fig. 7. Morphology of corrosion attack of copper electrode with addition of $FeSO_4$ 10^{-4} M at various polarisation potentials: (A) −0.90 V (SCE); (B) −1.00 V; (C) −1.10 V; (D) −1.25 V.

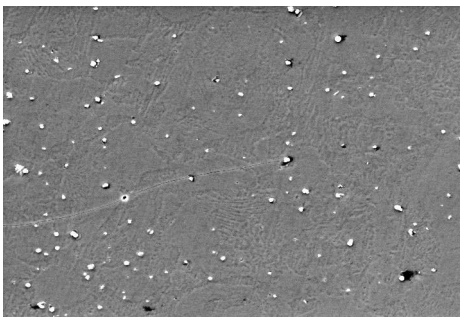

Fig. 8. Morphology of corrosion attack of carbon steel electrode in pure solution.

1–4A, solid line): the first one from about 0.0 V, after the current maximum, up to −0.1 V, the second, wider one from −0.15 to −0.4 V/SCE. This latter appears also in the presence of iron sulphate (Figs. 1–4A, dotted line).

The *iron sulphate addition* changes significantly the copper electrode behaviour. The high peak at $0.02 \div 0.12$ V disappears in the first direct scan as if the iron ions inhibited the formation of the copper compounds that give rise to the peak. Nevertheless the same peak reappears in the subsequent cycles with lower and lower currents when increasing IP (Figs. 1–4C, dotted line). On the contrary, the potential values of the second range of oscillations can be located in all the curves. Furthermore at the IP of −1.25 V, the reverse scans, unlike those in pure solution (Fig. 4B and D), show always a high desorption peak, shifted towards less noble potentials ($-0.75 \div -0.80$), which is immediately followed by a reduction peak. Such a peak, observed also on steels electrodes (Fig. 5B) suggests that the iron system interferes with the copper–chromium system giving rise to more stable compounds.

Acknowledgements

The studies here presented, form a part of an Italian National Research Project entitled ‘Leghe e composti intermetallici. Stabilità termodinamica, proprità fisiche e reattività’. The authors are grateful to the Italian Ministero dell’Università e della Ricerca Scientifica e Tecnologica (Programmi di Ricerca Scientifica di Rilevante Interesse Nazionale) and the O.C.S. Group for financial support

References

[1] C.G. Fink, US Patent 1,581,188 (1926).
[2] J.P. Hoare, J. Electrochem. Soc. 126 (1979) 190.
[3] A.G. Mokov, N.A. Karnaev, Elektrokimiya 21 (1985) 217.
[4] L.N. Solodkova, Z.A. Solov’eva, Elektrokimiya 11 (1975) 1669.
[5] L.N. Solodkova, Z.A. Solov’eva, Elektrokimiya 15 (1979) 106.
[6] J.P. Saiddington, G.R. Hoey, J. Electrochem. Soc. 117 (1970) 1012.
[7] J.P. Saiddington, G.R. Hoey, J. Electrochem. Soc. 120 (1973) 1475.
[8] Y.V. Kondrashov, Z.A. Solov’eva, Elektrokimiya 26 (1990) 217.
[9] E. Soragni, P. Mazzeo, C. Fontanesi, Mater. Eng. 8 (1997) 321.
[10] E. Soragni, C. Fontanesi, G. Barani, V. Ganzerli, J. Appl. Electrochem. (submitted).
[11] M. Pourbaix, Atlas of Electrochemical Equilibria in Aqueous Solutions, Pergamon Press, London, 1966.